

A Wireless Energy Transfer Platform, Integrated at the Bedside

Hans De Clercq, *Student Member, IEEE* and Robert Puers, *Fellow, IEEE*

Abstract—This paper presents the design of a wireless energy transfer platform, integrated at the bedside. The system contains a matrix of identical inductive power transmitters, which are optimised to provide power to a wearable sensor network, with the purpose of wirelessly recording vital signals over an extended period of time. The magnetic link, operates at a transfer frequency of 6.78MHz and is able to transfer a power of 3.3mW to the remote side at an inter-coil distance of 100mm. The total efficiency of the power link is 26%. Moreover, the platform is able to dynamically determine the position of freely moving sensor nodes and selectively induce a magnetic field in the area where the sensor nodes are positioned. As a result, the patient will not be subjected to unnecessary radiation and the specific absorption rate standards are met more easily.

I. INTRODUCTION

Recent progress in the field of intelligent body sensor networks has enabled the application of wearable devices to clinical treatment [1]. Since these systems supersede bulky bedside monitors and bypass wires, hampering the patients movement, they emphasize an increase of comfort and facilitate long-term biosignal acquisition. Moreover, these devices facilitate an effective rehabilitation period in a home environment, which is not only beneficial to the patients well being, but also stimulates cost-effectiveness in global health. Modern diagnostics, however, implicate long-term, high-quality data acquisition. Consequently, these medical body sensor networks are dealing with a challenging trade-off between signal quality, miniaturization and autonomy. Inductive power transfer overcomes the shortage of on-board available energy and is efficient enough to avert such a compromise. This technique, referred to as transcutaneous energy transfer (TET), is already widely used in the field of medicine to bias medical implants [2], [3], [4]. But also wireless non-invasive devices, used for bedside monitoring, can benefit from a wireless magnetic link. In that case, the system consists of a fixed, primary coil in the bed, and one or more remote monitoring units attached to the patient. In contrast to transcutaneous energy transfer, which typically corresponds to a relatively high and fixed coupling factor, inductive powering at the bedside implies loosely coupled coils with significant variations due to patient movement. In previous work a life-sized clinical setup, based on a Helmholtz configuration, was devised to deal with similar coupling fluctuations [5]. The resulted magnetic field was proven to be homogeneous within a constrained working

We acknowledge the institute of the Promotion of Innovation through Science and Technology in Flanders (IWT-Vlaanderen).

H. De Clercq and R. Puers are with the Division Microelectronics and Sensors (MICAS), Department of Electrical Engineering (ESAT), Katholieke Universiteit Leuven, Arenberg 10, B-3001 Heverlee, Belgium. hans.declercq@esat.kuleuven.be

volume of $0.18m^3$; nevertheless in this manner, the full upper body part of the patient is exposed to the magnetic field. This paper introduces a matrix of primary coils at the bedside, which can dynamically determine the positions of the remote sensor nodes and radiate selectively, so that the patient will not be subjected to unnecessary radiation and the specific absorption rate standards [6] are met more easily. While previous work has demonstrated an online control system to repress power fluctuations due to vertical coil displacement [7], this work will focus merely on horizontal changes.

II. HIGH-LEVEL SYSTEM DESIGN

A. The Overall System Architecture

A block-level schematic of the overall system is illustrated in fig. 1. The on-body part consists of a sensor network for biosignal acquisition. In addition to the sensor interface, each node contains a microcontroller for data management and a 2.4GHz-link for RF-networking. The power consumption of the sensor node is less than $3.3mW$ at a voltage of $3.3V$. Each module is surrounded by a helical coil and incorporates energy scavenging circuitry for the magnetic link [8]. The off-body part, which is integrated into the bed, contains a matrix of identical inductive power transmitters. The amplifiers are built up with off-the-shelf components, and are driven by a 6.78MHz pulse modulated signal, generated by a microcontroller with a clock speed of 54.24MHz. A power MOSFET driver is included to adequately drive the amplifier.

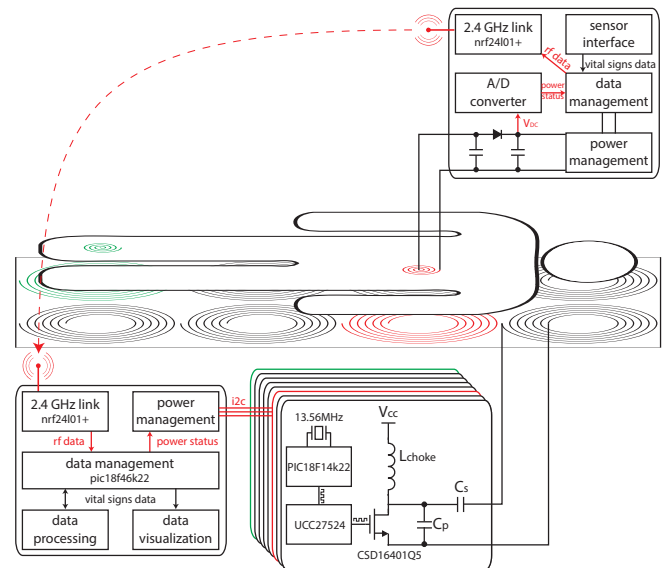


Fig. 1. A block-level schematic of the overall system.

A centralized data management unit gathers the medical data and is in charge of signal processing and visualization. It can communicate with a maximum of six wearable sensor nodes and creates the possibility to online adjust data acquisition parameters. This main unit also administers the wireless power transfer of the multiple power transmitters through I^2C -communication.

B. Online Power Link Control using RF communication

Fig. 1 shows two nodes, attached to the patient, which are powered through two separate power links. Instead of creating a homogeneous magnetic field within the working space of the remote system, the off-body management unit is able to determine the position of each sensor node and selectively induce a magnetic field in the area where the sensor nodes are situated. Selective radiation will not only be beneficial for patient safety, but will also increase link efficiency. At a given height within a confined space, we can indeed presume that there will always be a base coil that is most optimally coupled with the remote side. Moreover, in case of multiple sensor nodes, online power optimization techniques such as discussed in previous work [7] can concurrently be applied to the different power transmitters. In the consumer market, similar energy transfer systems are rapidly gaining momentum, enabling a convenient new way to charge mobile devices. This resulted in the establishment of the Wireless Power Consortium and the introduction of the Qi standard for low-power inductive charging [9]. Nevertheless, this standard has several shortcomings when applied to bedside patient monitoring. Firstly, in case of mobile device charging, we can assume that the inductive coupling will remain constant after an initialization phase. Secondly, the Qi standard is devised for a close and stable inter-coil spacing, which makes it possible to use backscatter modulation as a communication technique [10]. To cope with the loosely coupled link and constant patient and sensor movement, in case of bedside monitoring, the high-data-rate RF-Link, which already conducts the medical data transfer, is used to administer the power links. To dynamically determine the position of freely moving sensor nodes, the received power is constantly monitored at the remote side by measuring the induced rectified voltage. The power data of the different nodes is concurrently communicated to the data management unit at a sample rate of 10sps . Software has been developed to calculate which of the different coils needs to be activated to provide the sensor with optimal power. In an initialization phase, every coil needs to be toggled on and off, one by one. During this phase the most efficient magnetic power amplifier is determined for each subjected sensor node. After initialization the induced voltage is constantly monitored. As long as this voltage lies between $3V$ and $4.5V$, the magnetic transmission unit is not interchanged. In case of lower induced voltages the search procedure restarts determining the best candidate, beginning with the adjoining transmitters. In case of higher induced voltages, the system is shut down and an alarm is given.

III. INDUCTIVE LINK OPTIMIZATION

For a constant remote coil height, the proposed technique enables link optimisation, which further minimizes patient exposure to the magnetic field. Such an optimization strategy of a loosely coupled inductive link can be subdivided into two parts: the magnetic design; optimizing the link efficiency for given coil sizes, coil separation and frequency, and the electronic design; tuning the additional circuitry to efficiently drive a considerable a.c. current into the base coil [11].

A. The Magnetic Design Procedure

The magnetic design implies the construction of a set of coils that optimally fits to the given load. The radius of the remote solenoid inductor is 8.5mm and is determined by the size of the sensor module. A coil separation of 100mm is appointed and the maximum size of each flat spiral primary inductor is limited to 150mm . The procedure starts with the design of the primary coil. This design implies a trade-off between a high coil quality factor, which benefits the link efficiency, and a limited coil inductance, to reduce the voltages at the primary side. Keeping this in mind, a spiral base coil, consisting of twelve windings with a gradually increasing diameter between 48mm and 144mm is constructed. This results in a total inductance of $14.8\mu\text{H}$. For these dimensions we calculated the coupling factor, k to be 0.28% . At low frequencies, the effective series resistance of the base coil can be approximated as the d.c. resistance. However, at higher frequencies, the a.c. resistance, due to the skin effect and proximity effect should be taken into account. To minimize these effects, the coils are wound using Litz-wire from New England Wire Company with strands of $AWG48$. In this case, the effective series resistance is given by [12]:

$$ESR = R_{DC} \left(1 + K_c \left(\frac{N_s ID}{OD} \right)^2 \left(\frac{ID \sqrt{f}}{0.262} \right)^4 \right), \quad (1)$$

where R_{DC} is the DC resistance, N_s is the number of strands, K_c is a constant depending on the number of strands, ID is the diameter of a single strand and OD is the Litz wire diameter. The base coil resistance at 6.78MHz is calculated to be 0.31Ω , which gives a base coil quality, of 2026. The remote coil will be designed to maximize the link efficiency for an output power of 3.3mW and an output voltage of $3.3V$, which corresponds to the needs of the remote sensor nodes. The efficiency of a magnetic link defined as the ratio of the useful power dissipated in the a.c. load at the remote side to the power put into the inductive link at the base side, is given by:

$$\eta_{link} = \frac{k^2 Q_{base} Q_{rem}^2}{\left(1 + \frac{Q_{rem}}{\alpha} + k^2 Q_{base} Q_{rem} \right) (\alpha + Q_{rem})}, \quad (2)$$

where k stands for the coupling factor, Q_{base} and Q_{remote} are the quality factors of respectively the base coil and the remote coil and

$$\alpha = 2\pi f C_2 R_{a.c.} \quad (3)$$

corresponds to the ratio of the a.c. load to the reactance of the parallel resonance capacitor at the remote side. The link power losses are mainly determined by the parasitic resistances of the base and remote coils. The base coil efficiency is given by:

$$\eta_{base} = \frac{k^2 Q_{base} Q_{rem}}{1 + \frac{Q_{rem}}{\alpha} + k^2 Q_{base} Q_{rem}}, \quad (4)$$

and the remote coil efficiency is given by:

$$\eta_{rem} = \frac{Q_{rem}}{\alpha + Q_{rem}}. \quad (5)$$

The total link efficiency can be optimized for given quality and coupling factors to an optimal α -value [11]:

$$\alpha_{opt} = \frac{Q_{rem}}{\sqrt{1+X}}, \quad (6)$$

where

$$X = k^2 Q_{base} Q_{rem}. \quad (7)$$

This value can be found by choosing a realistic remote quality factor as an initial value. The associated optimal remote inductance can then be calculated via the parallel resonance capacitor, link frequency and given load. Next, the real quality factor can be derived by calculating the number of windings, needed to approximate the optimal inductance, and the effective series resistance of these windings. This optimization process can then be iterated using the derived quality factor as a new initial value. For the given load, an optimal remote inductance of $470nH$ and remote quality factor of 353.5 is found. This corresponds to a link efficiency of 44%. The rms-value of the induced magnetic field, which is given by [5]:

$$H = \frac{V_{rem}}{N_{rem} \pi^2 a^2 2f \mu_0} \quad (8)$$

is $55.3A/m$. This corresponds to a magnetic flux density of $69.5\mu T$. These values are below the ICNIRP reference levels for occupational exposure to magnetic fields [6].

B. The Electronic Design Procedure

A class-E driver is selected to drive the base coil. The selected power MOSFET operates as an on/off switch and the load network shapes the voltage and current waveforms to prevent simultaneous voltage over and current through the transistor. This driver exhibits high efficiencies even at high frequencies, due to zero turn-on voltage characteristics [13].

However, generally, closed-loop circuits have to be foreseen to actively compensate unstable operation due to coupling and load variations [14], [15]. This phenomenon particularly exists for well-coupled systems, while in case of loose coupling the ensued variations mainly cause voltage fluctuations at the secondary side [7]. A duty cycle of 25% is chosen to minimize the required supply current. Fig. 3 depicts the Spice simulation results. The top graph shows the drain-to-source voltage, V_{DS} , in the case that an ideal switch replaces the power MOSFET. The graph clearly indicates that the drain-to-source voltage is zero when the switch is

open. The second graph shows the same result, in which extra losses due to the power MOSFET are introduced. Also, off-the-shelf capacitance values are chosen, which gives rise to an additional deficiency. The class-E amplifier has an efficiency of 87%. The total efficiency of the system is 33%. Fig. 2 indicates the different power losses of the total system.

Table I summarizes the results of the magnetic and electronic design procedures.

IV. SYSTEM IMPLEMENTATION AND RESULTS

A bedside coil matrix, containing eight identical base coils is developed. The spiral coils are mounted on a $600mm$ by $300mm$ plate of Plexiglass. To enhance coil winding, the ideal spiral contour is engraved into the plate, using a laser cutter. The measured inductance corresponds to the calculated value of $14.8\mu H$, but a variation of $100nH$ is encountered within the eight coils. The CSD16401Q5 power MOSFET and UCC27524 MOSFET driver are chosen to drive the class-E. The realised coil matrix and the corresponding power transceiver circuit board can be observed in fig. 4. To show system feasibility, the prototype is used to power the body-sensor network, detailed out in [8]. The real coupling factor approximated the simulated value, but the total efficiency, not taking into account the microcontroller and driver power losses, dropped to 26%. This decrease in power efficiency is a result of capacitance mismatch, which detunes the class-E regime and the resonance tank at the remote side. The software algorithm, used to determine the position of the sensor nodes and to control the wireless power platform has been integrated into the centralized management unit and is successfully tested. Future work will focus on the expansion of the online power optimization algorithm by adding voltage control in case of vertical inter-coil displacements[7] and on extending the inter-coil distance. Furthermore, the calculated magnetic field strength needs to be verified.

V. CONCLUSION

The presented research has introduced an inductive energy transfer platform integrated at the bedside. It consists of a matrix of transmitting coils, covering an area of $0.18m^2$. A software algorithm, which can automatically assign the most efficient power transmitter to bias a freely moving remote sensor node, has been developed. Experiments have proven the systems aptitude to deal with online horizontal sensor movement. Effort has been put in the design, simulation

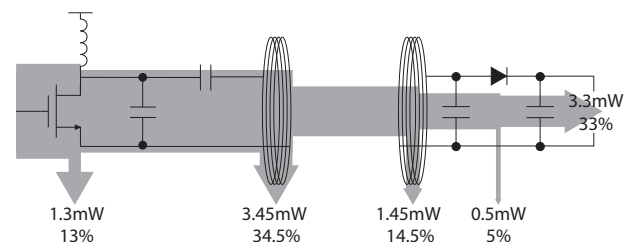


Fig. 2. The power distribution in the inductive link.

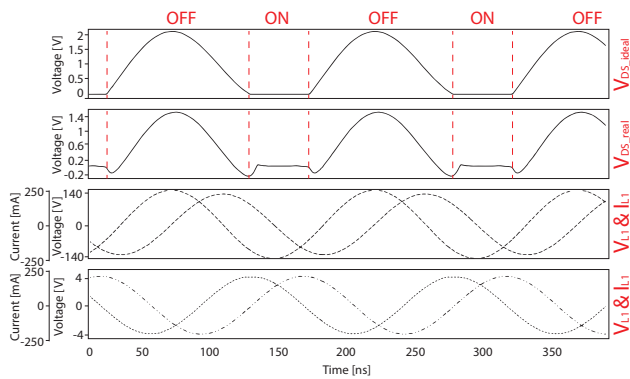


Fig. 3. Spice simulations of the dedicated class-E driver.

and implementation of a highly efficient, loosely coupled inductive link. The system makes it possible to provide $3.3mW$ to a remote node at an inter-coil distance of $100mm$ out of a $12.7mW$ -power supply. Such a system enables wirelessly recording vital signs over an extended period of time at the bedside. Moreover, the induced magnetic field is $55.3A/m$ and the corresponding magnetic flux density is $69.5\mu T$. These values are below the ICNIRP reference levels for occupational exposure. Therefore, this method increases patient safety compared to previous work and justifies inductive powering as a method for long-term bedside observation.

REFERENCES

- [1] P. Bonato, Wearable sensors/systems and their impact on biomedical engineering, IEEE Engineering in Medicine and Biology Magazine, vol.22, no. 3, pp. 18-20, 2003.
- [2] L. Zhao, C.F. Foo, K.J. Tseng, and W.K. Chan, "Transcutaneous transformers in power supply system for an artificial heart," in International Conference on Power Electronic Drives and Energy Systems for Industrial Growth, pp. 348 - 352, 1998.

TABLE I

MAGNETIC AND ELECTRONIC DESIGN SUMMARY

Magnetic Design		Electronic Design	
Parameter	Value	Parameter	Value
output power [mW]	3.3	parallel cap [nF]	3.5
output voltage [V]	3.3	serial cap [pF]	37.5
frequency [MHz]	6.78	choke [nH]	330
inter coil spacing [mm]	100	supply voltage [V]	0.5
base inductance [μH]	14.8	supply current [A]	0.02
base quality factor	2026	ds voltage [V_{max}]	2.2
base resistance [Ω]	0.31	ds current [A_{max}]	0.5
base windings	12	base voltage [V]	100
remote inductance [μH]	0.47	base current [A]	0.18
remote quality factor	353.5	remote voltage [V]	2.8
remote resistance [Ω]	0.06	remote current [A]	0.14
remote windings	4	diode threshold [V]	0.5
alpha	136.1		
resonance cap [nF]	1.2		
link coupling [%]	0.28		
base efficiency [%]	61	class-E efficiency [%]	87
remote efficiency [%]	72	rect. efficiency [%]	87
link efficiency [%]	44	total efficiency [%]	33

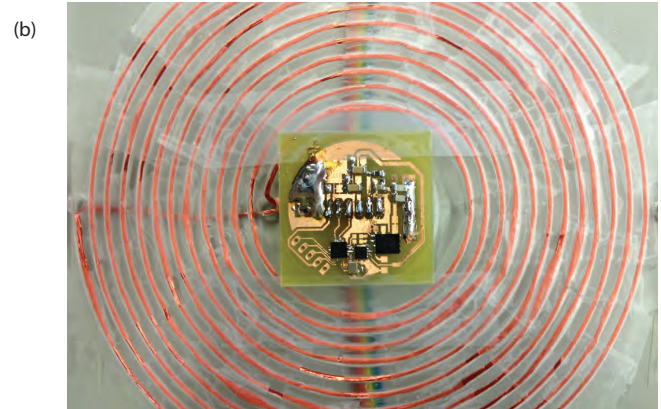
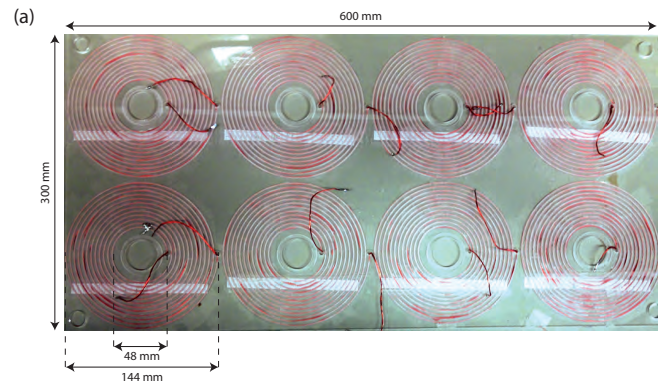


Fig. 4. (a) The wireless energy transfer platform prototype. (b) The class-E power transceiver circuit for one inductive link

- [3] M.W. Baker, and R. Sarpeshkar. Feedback analysis and design of RF power links for low-power bionic systems. IEEE Transactions on Biomedical Circuits and Systems, vol. 1, pp. 28-38, 2007.
- [4] G. A. Kendir, W. Liu, G. Wang, M. Sivaprakasam, R. Bashirullah, M. S. Humayun, and J. D. Weiland, An optimal design methodology for inductive power link with class-E amplifier, IEEE Trans. on Circuits and Systems I, vol. 52, pp. 857-866, May 2005.
- [5] P. Jourand, and R. Puers, A Class-E driven inductive power delivery system covering the complete upper body, Sensors and Actuators A: Physical vol.183, pp. 132-139, 2012.
- [6] ICNIRP, "Guidelines for limiting exposure to time-varying electric and magnetic fields," Health Physics 99(6), pp. 818-836, 2010.
- [7] H. De Clercq, and R. Puers, An Inductive powering system with online power optimization, using RF power feedback, In proceedings of the 19th symposium of the International Society on Biotelemetry, pp. 10-12, 2012.
- [8] H. De Clercq, and R. Puers, A Neonatal Body Sensor Network for Long-term Vital Signs Acquisition, Proc. Eurosensors, vol. 47, pp. 981-984, 2012
- [9] <http://www.wirelesspowerconsortium.com> (last accessed February 2013).
- [10] B. Lenaerts, and R. Puers, Omnidirectional Inductive Powering for Biomedical Implants, Berlin:Springer, 2008.
- [11] K. Van Schuylenbergh, and R. Puers, Inductive Powering. Analog Circuits and Signal Processing, XVI. Springer, 2009.
- [12] F. E. Terman, Radio Engineers Handbook. New York: McGraw-Hill, 1943.
- [13] N. Sokal, Class-E RF Power Amplifiers, QEX Commun. Quart p9-20, 2001.
- [14] R. Carta, J. Thon, G. Gosset, G. Cogels, D. Flandre, and R. Puers, A Self-Tuning Inductive Powering System for Biomedical Implants, Proc. Eurosensors, vol. 25, pp. 1585-1588, 2011.
- [15] P. R. Troyk, and M. A. K. Schwan, Closed-loop class E transcutaneous power and data link for MicroImplants IEEE Trans. Biomed. Eng., vol. 39, no. 6, Jun. 1992.